



HAL
open science

Recent Trends in the Recurrence of North Atlantic Atmospheric Circulation Patterns

Pascal Yiou, Julien Cattiaux, Aurélien Ribes, Robert Vautard, Mathieu Vrac

► **To cite this version:**

Pascal Yiou, Julien Cattiaux, Aurélien Ribes, Robert Vautard, Mathieu Vrac. Recent Trends in the Recurrence of North Atlantic Atmospheric Circulation Patterns. *Complexity*, 2018, 2018, pp.1-8. 10.1155/2018/3140915 . hal-02326190

HAL Id: hal-02326190

<https://hal.science/hal-02326190>

Submitted on 2 Jul 2021

HAL is a multi-disciplinary open access archive for the deposit and dissemination of scientific research documents, whether they are published or not. The documents may come from teaching and research institutions in France or abroad, or from public or private research centers.

L'archive ouverte pluridisciplinaire **HAL**, est destinée au dépôt et à la diffusion de documents scientifiques de niveau recherche, publiés ou non, émanant des établissements d'enseignement et de recherche français ou étrangers, des laboratoires publics ou privés.

Research Article

Recent Trends in the Recurrence of North Atlantic Atmospheric Circulation Patterns

Pascal Yiou ¹, Julien Cattiaux,² Aurélien Ribes,² Robert Vautard,¹ and Mathieu Vrac¹

¹Laboratoire des Sciences du Climat et de l'Environnement, UMR 8212 CEA-CNRS-UVSQ, IPSL & U Paris-Saclay, CE l'Orme des Merisiers, 91191 Gif-sur-Yvette Cedex, France

²Centre National de Recherches Météorologiques, UMR 3589 CNRS-Météo-France, 42 avenue G. Coriolis, 31057 Toulouse, France

Correspondence should be addressed to Pascal Yiou; pascal.yiou@lscce.ipsl.fr

Received 8 August 2017; Revised 7 December 2017; Accepted 11 January 2018; Published 12 February 2018

Academic Editor: Daniela Paolotti

Copyright © 2018 Pascal Yiou et al. This is an open access article distributed under the Creative Commons Attribution License, which permits unrestricted use, distribution, and reproduction in any medium, provided the original work is properly cited.

A few types of extreme climate events in the North Atlantic region, such as heatwaves, cold spells, or high cumulated precipitation, are connected to the recurrence of atmospheric circulation patterns. Understanding those extreme events requires assessing long-term trends of the atmospheric circulation. This paper presents a set of diagnostics of the intra- and interannual recurrence of atmospheric patterns. Those diagnostics are devised to detect trends in the stability of the circulation and the return period of atmospheric patterns. We detect significant emerging trends in the winter circulation, pointing towards a potential increased predictability. No such signal seems to emerge in the summer. We find that the winter trends in the dominating atmospheric patterns and their recurrences do not depend of the patterns themselves.

1. Introduction

Recent North Atlantic winter and summer extremes have been associated with persistent patterns of atmospheric circulation. Those patterns have been rather contrasted from one year to another. Cold spells of January 2010, December 2010, and February 2012 in Europe resulted from persisting blocking situations over Scandinavia [1, 2]. Warm winter 2006/2007 [3, 4] and stormy winter 2013/14 [5, 6] were dominated by persistent high-pressure systems over the Azores and the Mediterranean Sea, respectively. The warm summers of 2003 and 2015 in Europe were associated with either a persisting blocking pattern over Scandinavia or Atlantic low conveying warm air into Europe from North Africa. Therefore it is difficult to claim that a given atmospheric pattern has dominated during recent years to create such climate extremes. However it has been speculated that the amplitude of atmospheric patterns is changing, in particular through a connection between Arctic sea-ice cover and meanders of the jet stream [7, 8]. The statistical significance of such a trend as well as the relevance of the evoked mechanisms has been debated [9–11].

The midlatitude atmospheric variability is characterized by a baroclinic instability of the zonal flow [12]. This instability grows into Rossby waves. It has been argued that the excitation conditions of those Rossby waves have increased in the past decades [8, 13].

Faranda et al. [14] studied how unstable fixed points of the extratropical atmospheric circulation correspond to blocking patterns of the circulation. Faranda et al. [15] investigated the local dimension of North Atlantic atmospheric circulation and examined the implications for predictability in the winter season. The local dimension is linked to the recurrence properties of a complex system [16–18].

In this paper, we analyze recently observed trends in the surface North Atlantic circulation in winter and summer. We focus on recurrences of patterns of the atmospheric circulation [16, 19]. We examine trends in the intraseasonal recurrence of flow patterns by using the notion of recurrence networks within a season, as introduced by Donner et al. [20]. The trend in interannual pattern recurrence is examined through the probability of detecting good analogues of circulation. Those intra- and interannual diagnostics allow detecting emerging properties of the atmospheric circulation.

2. Data and Methods

2.1. Data. We use the reanalysis data of the National Centers for Environmental Prediction (NCEP) [21] between January 1948 and March 2017. We consider the sea-level pressure (SLP) over the North Atlantic (80W–30E; 30–70N). One of the caveats of this reanalysis dataset is the lack of homogeneity of assimilated data, in particular before the satellite era. This can lead to breaks in pressure related variables, although such breaks are mostly detected in the southern hemisphere and the Arctic regions [22]. A multiple breakpoint detection algorithm [23] was applied to the time series we generate, in order to determine whether our results depend on the assimilated data of the reanalysis. No breakpoint was detected at or near the years of introduction of satellite data in the reanalysis (not shown).

The SLP field structure contains a seasonal cycle that needs to be removed. We computed seasonal anomalies of SLP. For each grid point of the reanalysis, a daily seasonal cycle is computed with a smoothing spline of daily averages, with a differentiability constraint at December 31 and January 1. The mean seasonal cycles obtained at each gridpoint are subtracted to the time series of SLP in order to produce anomalies of SLP.

2.2. Intraseasonal Recurrence. The first concept we develop is the intraseasonal recurrence of atmospheric patterns for the winter and summer seasons (December-January-February (DJF) and June-July-August (JJA)). The temporal autocorrelation (number of days with an autocorrelation significantly above 0) of SLP around the North Atlantic is close to 5 days on average [24]. If the atmospheric circulation fluctuates around a given state on time scales that are longer than 5 days, this might not be reflected by the sample autocorrelation. Beyond the *persistence* defined by “remaining in a pattern during consecutive times,” we are interested in the fact that the atmosphere could come back to a given pattern, after a significant disturbance. This identifies a recurrent—although unstable—state of the atmosphere, potentially corresponding to a wave excitation. This state does not need to be the same from one year to another. In this subsection we adopt two ways of measuring the intraseasonal recurrence of patterns within a season.

The first one is based on the analysis of weather regimes of the atmospheric circulation. For each season, the SLP anomalies (with respect to the seasonal cycle) are classified onto four weather regimes. This number corresponds to what is usually found in the literature [25–27]. We compute the principal components (PCs, [28]) of the NCEP reanalysis SLP anomaly data. SLP data is weighed by the cosine of latitude for the computation of PCs/EOFs. The weather regimes (WR) are determined by a k -means clustering of the first 10 PCs, between 1970 and 2000 [27, 29].

For each year and each season (winter and summer, between 1948 and 2017), the daily SLP anomaly patterns are attributed to the closest WR pattern (in terms of Euclidean distance to the cluster mean). The annual *frequency* of WR is the ratio of number of occurrences of the WR to the length of the season. For each year and each season, the dominant

WR is the one with the highest frequency, and we report the frequency of the dominant weather regime.

The second approach to that concept of intraseasonal recurrence is based on the similarity of intraseasonal daily SLP anomaly patterns. For each reference day d within a season, we determine all the days d' of the same season that yield a spatial rank correlation r that exceeds a threshold r_0 . Here, we take $r_0 = 0.5$, which corresponds to the 60th percentile of all intraseasonal sample correlation values. We construct a *network* of analogue days $S(d, y)$, for all days d in years y by

$$S(d, y) = \{d' \in y, r(\text{SLP}_d, \text{SLP}_{d'}) \geq r_0\}. \quad (1)$$

The days in $S(d, y)$ fall in the same season (DJF or JJA). The so-called “dominating” network $S(y)$ is the one that yields the largest number of analogue patterns. This network definition is similar to the recurrence network of Donner et al. [20]. We consider the number of days in the dominating analogue network and the frequency (percentage of days) within a season. We call this percentage of days the *frequency* of the $S(y)$ analogue network (or $S(y)$ for short).

This approach is akin to the dominating WR analysis, but it does not constrain the geographical location of the predefined weather patterns. The fluctuations of the frequencies of the dominating WR or the $S(y)$ network help us assess how the persistence of atmospheric patterns varies through time. Those two intraseasonal quantities (frequencies of dominating weather regime and dominating network) allow investigating recurrent but potentially unstable patterns of the atmospheric circulation. Those patterns do not need to be visited in spates of consecutive days.

Those two approaches are meant to determine the trend of intraseasonal pattern recurrence. The choice of $r_0 = 0.5$ is justified a posteriori by comparing the values of the frequency of the network $S(y)$ and the frequency of the dominating WR. If the threshold correlation r_0 increases, the size of $S(y)$ decreases. A value of $r_0 = 0.6$ divides size of $S(y)$ by 2 and gives a range of variations that is much smaller than the average value of the dominating WR frequency, which leads to a more difficult physical interpretation.

We emphasize that this concept of intra-annual network recurrence is distinct from the clustering index examined by Faranda et al. [15], which focuses on the local persistence of the system. But the concept is complementary to the analyses of Faranda et al. [14] because we identify regions in the phase space of the atmospheric circulation to which trajectories “try” to come back close to.

2.3. Interannual Recurrence. The second concept we use is the interannual recurrence of SLP patterns. In contrast with the previous definitions, the *interannual* recurrence in atmospheric sciences [e.g., [16]] based on events that occur in *different* years but the same season, in order to ensure statistical independence. The time evolution of the (inter-annual) recurrence properties (e.g., in terms of closeness or return time) provides information on trends in the dynamics of the system [18, 30]. Such trends suggest the emergence of patterns.

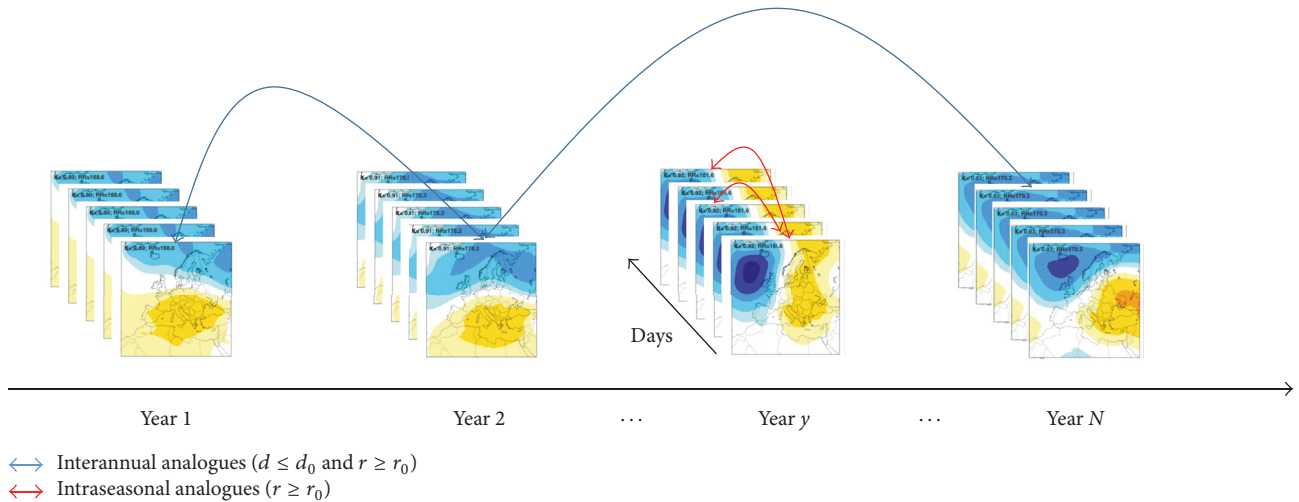


FIGURE 1: Schematic representing how the intraseasonal analogues (red lines) and the interannual analogues (blue lines) are determined from SLP fields.

In this paper, the long-term emergence (or disappearance) of patterns is estimated from interannual analogues of circulation [4, 16]. For each day, we determine the best 20 analogues of circulation by minimizing a Euclidean distance to all days occurring in a different year, but at most 30 calendar days apart. Good analogues have a distance that is smaller than a threshold d_0 corresponding to the 25th percentile of distance, and a spatial correlation that is higher than a threshold $r_0 = 0.5$ corresponding to the 75th percentile of spatial correlations of all 20 best analogues. In practice, the number of good analogues for a given day is always lower than 10 for such data. Therefore retaining more than the 20 best analogues would not change the results.

The distributions of correlations for interannual analogues (i.e., picked in another year) and intraseasonal analogues are different, which explains that the value $r_0 = 0.5$ corresponds to different quantiles in the two cases. The seasonal average number of good analogues is a proxy for the probability of observing a circulation pattern and gives access to the usual character of a season. If this number decreases, then one can conclude that the circulation during that season becomes less typical, leading to the appearance of new patterns with no past analogues.

The intraseasonal and interannual analogues (or recurrences) are illustrated in Figure 1. They are linked through recurrence diagrams [19]. The intraseasonal analogue networks are related to thickness of the diagonal lines of recurrence diagrams, when one considers short-term recurrences. The interannual analogues are related to off-diagonal properties of recurrence diagrams, when one considers longer term recurrences. The distinction we make simplifies the visualization of the analyses, as the two timescales (intra-annual versus interannual) refer to two timescales of a complex system that pertain to different types of behavior.

3. Results

3.1. Intraseasonal Recurrences. The frequency of the dominating $S(y)$ network pattern yields a positive trend in winter

(1% of winter days per decade, p value < 0.05) (Figure 2, dashed black lines) and a negative trend in summer (-1% of summer days per decade, p value < 0.001) (Figure 3, dashed black lines). The positive winter trend is unstable, due to the upward fluctuation in the 1990s: the trend since 1980 (the use of satellite data in the reanalysis) is close to 0 and not significant, and the trend since 1997 (with the optimal number of assimilated observations) is 1.3% per decade. The summer trend over 1950–2017 is also unstable, with negligible and insignificant trends since 1980 and 1997. The number of days spent in the summer dominating WR (≈ 38 days) or the dominating $S(y)$ network (≈ 20 days) is smaller than in the winter (resp., 40 days and 30 days). From a count of the dominant WR frequencies in Figure 2, the zonal weather regime (ZO) has been preferred in the winter between 1948 and 2015. The ZO weather regime corresponds to what is called NAO+ (or the positive phase of the North Atlantic Oscillation) in many papers. Since the NAO+ terminology has been used when referring to monthly SLP patterns, we prefer to adopt the ZO terminology, which refers to daily patterns [25, 31].

The ZO weather regime dominated 35% of winters (BLO: 29%; NAO-: 19%; AR: 16%). Those weather regimes have dominated winters roughly and equiprobably since 2000. The preferred summer weather regime (Figure 3) has been the Scandinavian Blocking (BLO: 40% of summers) (against NAO-: 21%; AR: 21%; AT: 18%). The summer Atlantic Ridge (AR) has dominated only once since 2000 and the other three weather regimes have been rather equiprobable. The AR weather regime is unlikely during warm summers [25]. The period since 2000 has been the longest spell with so few AR occurrences since 1948, although it is difficult to interpret the behavior of the last 15 years in terms of an emerging signal, because of the large decadal variability of the dominating regimes. A similar analysis of the 20CR reanalysis ensemble mean [32] provides the same results on the 1948–2012 period (not shown). The period before 1948 does not yield any significant trend, but this could be due to the large ensemble spread whose averaging smears out trends (not shown).

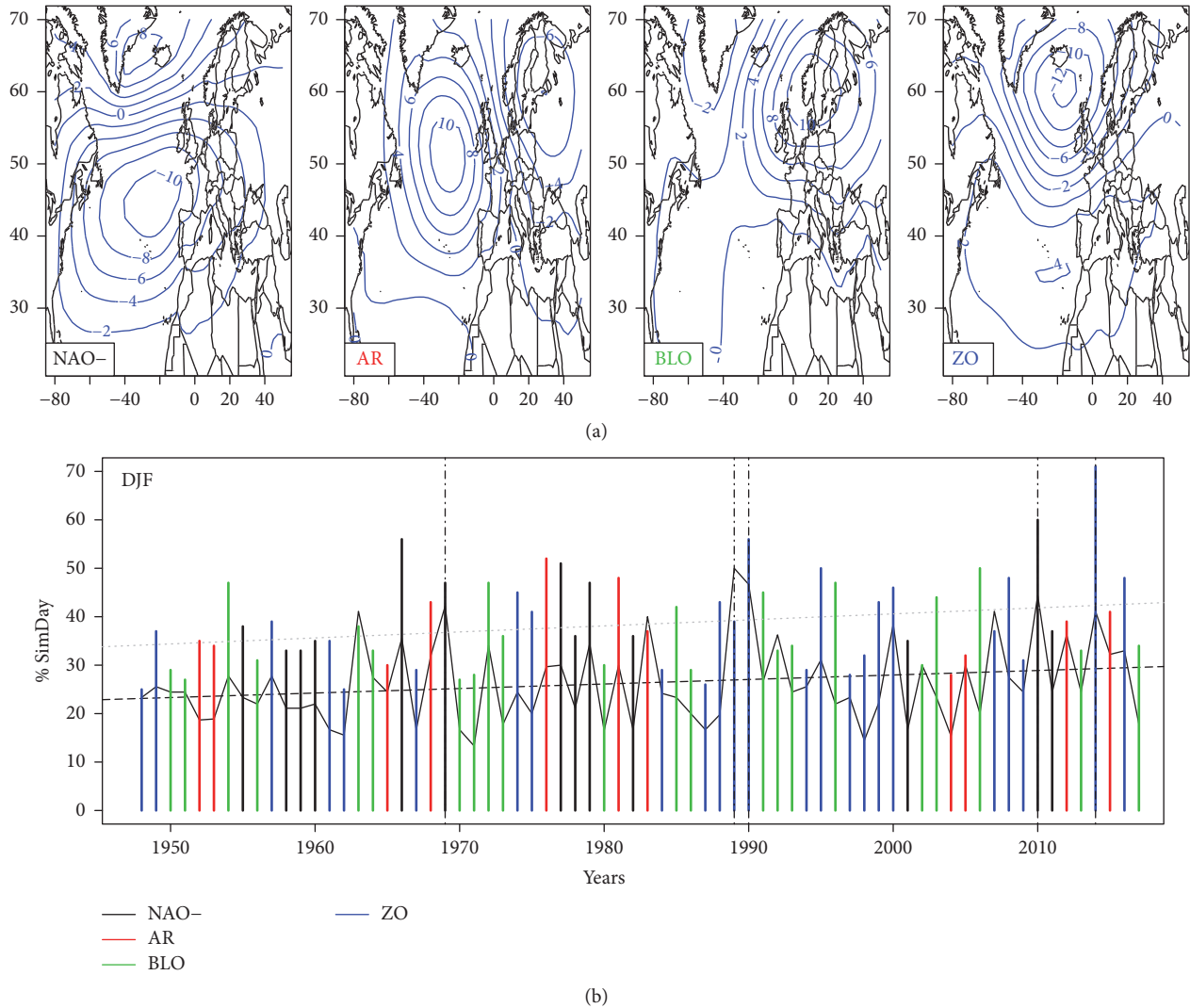


FIGURE 2: (a) Four weather regimes of SLP anomalies in DJF (negative phase of the NAO, Atlantic Ridge, Scandinavian Blocking, zonal flow). The isolines have increments of 2 hPa. (b) Trends in atmospheric persistence for DJF. Vertical colored lines: frequency of dominating weather regime. The color is associated with a weather regime (NAO-: black; AR: red; BLO: green; ZO: blue). Gray dotted line: linear trend of regime frequencies. Continuous back lines: frequency of dominating network in the winter. Dashed black lines: linear trend of dominating network frequency. Vertical dash-dotted lines are for the five years with the largest numbers of similar days (1969, 1989, 1990, 2010, and 2014).

We identify five winters with the largest frequencies of $S(y)$ networks (1969, 1989, 1990, 2010, and 2014). The SLP patterns for those years are shown in Figure 4. The winters that are identified yield zonal (1989, 1990, and 2014) or NAO- (1969 and 2010) weather regimes. We also find that the winters between 1948 and 2014 with more than 35 similar days are in one of those two weather regimes. The extremely persistent winter patterns are the two phases of the North Atlantic Oscillation that generate either stormy and warm surface conditions (ZO regime) or wet and cold conditions (NAO- regime) over Western Europe.

The five summers for which the recurrence is highest (larger than 25%) are mostly in the Atlantic Ridge regime (4 occurrences) and Scandinavian Blocking (1 occurrence) (Figure 3). By contrast, the five most frequent summer weather regimes (more than 45%) are the Scandinavian Blocking (3

occurrences), Atlantic Ridge (1 occurrence), and Atlantic Low (1 occurrence). This shows that the maximum occurrence of a weather regime within a season is disconnected from its interannual frequency: the summer AR regime is the most recurrent but is not very frequent. Such high recurrence values do not occur after 2000.

3.2. Interannual Recurrences. The average number of good circulation analogues characterizes the recurrence of the patterns in time. Hence, seasons with few good analogues can be considered as rare, while those with many good analogues are typical. A trend in the number of good analogues indicates a shift in the atmospheric circulation patterns, which might not be detectable in the frequency of weather regimes. Figure 5 shows the time variations of the mean number of good intraseasonal analogues for the summer

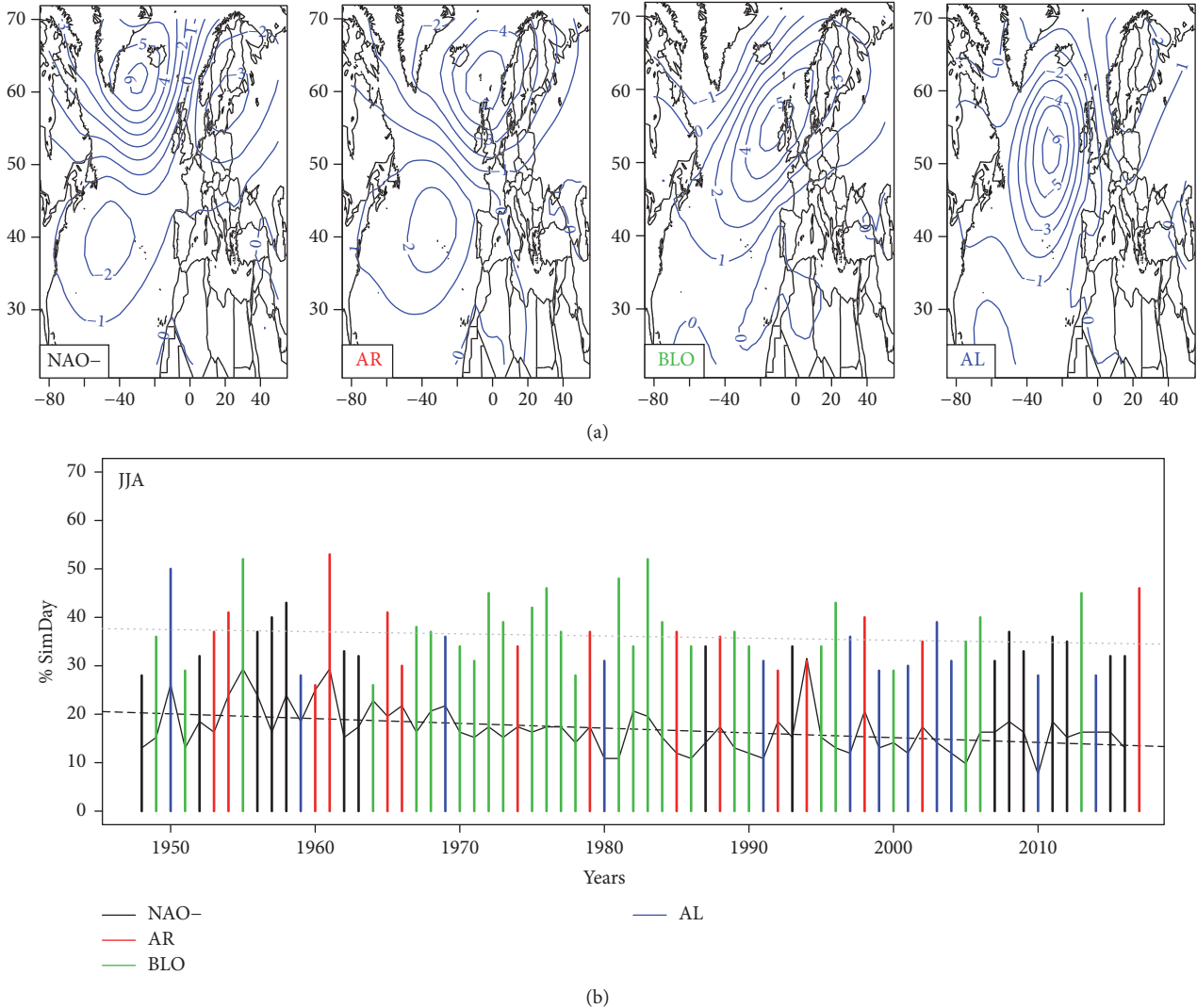


FIGURE 3: (a) Four weather regimes of SLP in JJA (negative phase of the NAO, Atlantic Ridge, Scandinavian Blocking, Atlantic Low). The isolines have increments of 2 hPa. (b) Trends in atmospheric persistence for JJA. Vertical colored lines: frequency of dominating weather regime. The color is associated with a weather regime (NAO-: black; AR: red; BLO: green; AT: blue). Gray dotted line: linear trend of regime frequencies. Continuous back lines: frequency of dominating network in the summer. Dashed black lines: linear trend of dominating network frequency.

and winter. The winter series yields a small but significant positive trend (0.1 analogue day per decade, p value < 0.01, Figure 5(a)). This means that the daily circulation patterns tend to become more frequent during the last decades, because the circulation analogues become increasingly good.

The summer series yields a significant negative trend (-0.07 analogue day per decade, p value < 0.01, Figure 5(b)). This means that the daily patterns have become individually more exceptional, although not necessarily extreme, from the first part of the period to the second part. The latter JJA decreasing trend does not hold for the last two decades (1990–2016), which yield a slightly positive trend. Therefore, this trend can hardly be interpreted in terms of a climate change signal, because it is likely to be influenced by decadal internal variability.

4. Discussion

As pointed out in the methods section, the value of the frequency of intraseasonal $S(y)$ analogue networks depends on the threshold correlation size of r_0 . A higher value (e.g., $r_0 = 0.6$) divides the average length by 2 and leads to a nonsignificant trend (p value > 0.05), especially for winter. But such a choice makes the comparison with dominating weather regimes harder to interpret, because the magnitudes of the variations (in Figure 2) would be too different.

The linear trend analysis can be challenged due to potential inhomogeneities in the NCEP reanalysis. As stated in Section 2.1, a breakpoint algorithm [23] was applied to the time series of dominating network and weather regime frequencies. One breakpoint in the mean occurs in 2005, which bears no inhomogeneity in the assimilation procedure of the

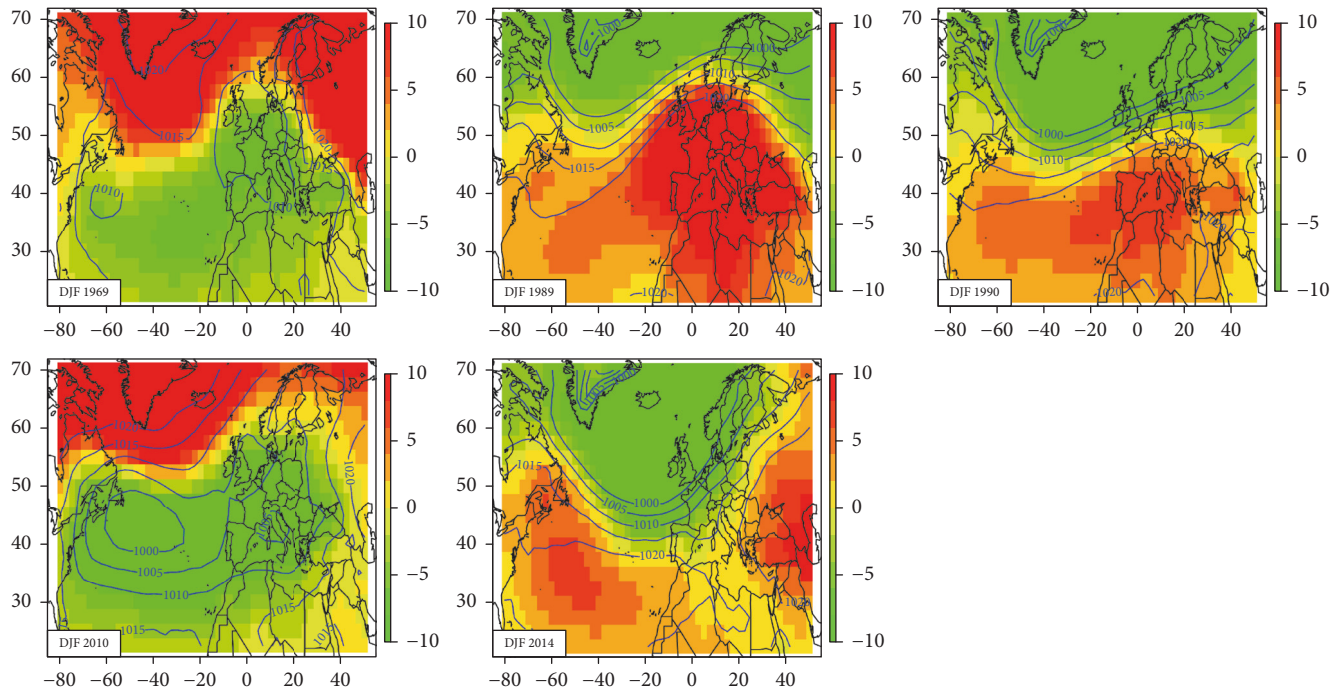


FIGURE 4: Composite of SLP for the recurrence networks for the five years outlined in the text (1969, 1989, 1990, 2010, and 2014). The isolines represent the SLP with increments of 5 hPa. The colors represent anomalies of SLP (in hPa) with respect to a mean seasonal cycle computed at each grid cell.

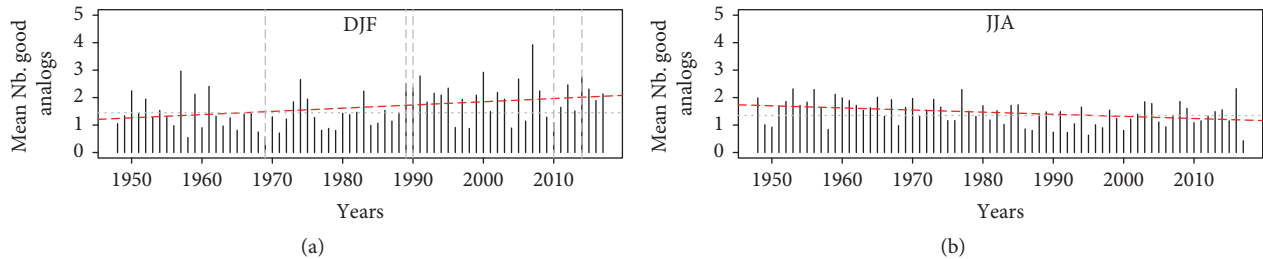


FIGURE 5: Average daily number of good analogues for the winter (DJF: panel (a)) and summer (JJA: panel (b)). The horizontal dotted lines indicate the mean value for all years. The red dashed line is the linear regression of the number of good analogues with time. The vertical dashed lines for panel (a) indicate the five reference winters (1969, 1989, 1990, 2010, and 2014).

reanalysis. We also fitted those time series a stepwise function with one break around 1979 (1975–1985), when satellite data start to be massively used. The fit is not significant (p value > 0.6 , not shown). This means that the significant linear trends we detect are not due to an inhomogeneity in the NCEP SLP data.

The increasing trend of similar atmospheric patterns in winter started only recently, in the 1970s (Figure 2). This trend means that the patterns become more frequent at the intraseasonal scale, with a locking to the phases of the North Atlantic Oscillation. Trends in the frequencies of those two weather regimes bring either prolonged episodes of snowfall to Europe (like in 2010, with an NAO– phase) or prolonged stormy episodes and precipitation episodes over Northern Europe (like in 2014, with zonal circulation). The concomitant increasing trend of the probability of finding a good winter circulation analogue (Figure 5) suggests that the return periods of observed winters become

shorter, so that winters tend to be similar to already known winters.

The decreasing trend of similar weather patterns in the summer means that slow building extreme events, such as droughts and heatwaves or cold summers, tend to be less frequent in Europe. The concomitant decreasing trend of interannual pattern recurrence suggests that summers become less similar to already known ones, although this trend is very small.

Those results can be interpreted in terms of an increase of predictability of the circulation in the winter because the size of the dominating network of weather patterns increases. There would be no such trend of predictability in the summer. Therefore, a prediction based on persistence would have an increased skill in the winter.

Our analyses seem to contradict the hypothesis of increased winter midlatitude atmospheric meandering described by Francis and Vavrus [7] and Petoukhov et al. [8],

because the winters with the most recurrent weather types we detect have had rather low wave numbers at the surface [33] while they were associated with extremely warm and stormy conditions (1989, 1990, and 2014) or extremely snowy conditions (1969, 2010) (Figure 4). Arctic sea-ice cover before those winters was either lower or above normal, and the meridional gradient of potential temperature did not show a systematic feature for those five cases, due to the fact that they correspond to opposite phases of the NAO. Yet, our analysis reaches similar conclusions on the impacts on European surface winter climate, in that more persistent zonal flows increase the probability of observing extratropical storms hitting Europe or extreme precipitation amounts in Northern Europe, as in 1999/2000 and 2013/2014. Conversely, prolonged spells of negative phase of the NAO in the winter increase the probability of extreme precipitation (including snow) in Southern Europe, as in 1969 and 2010. Our interpretation is that the atmospheric patterns that dominate during the winter tend to get “trapped” for longer times, although they are not necessarily more stable. We propose a conceptual model for this behavior, with an energy potential model in two dimensions with four wells whose relative depth varies randomly from one year to the next. Daily perturbations can force the system to shift wells, but at the end of the season, the deepest well is the most visited. We find that the deepest well becomes deeper in the winter.

The same analyses (persistence of SLP patterns) were performed for the North Pacific region and the whole Northern hemisphere extratropics (not shown). No trend is found on such regions and scales.

5. Conclusion

In this paper, we have shown significant, albeit small, emerging trends of recurrence properties of the atmosphere over the North Atlantic. Those trends point to increased atmospheric predictability in winter. This is coherent with the small decrease of local dimension reported by Faranda et al. [15]. The diagnostics we proposed have an interesting potential to assess the atmospheric temporal variability of climate models, especially for paleoclimates or future scenarios [34]. The *attribution* of extreme climate events (to climate change) requires decomposing an extreme event into its dynamical (linked to the atmospheric circulation) and thermodynamical (linked to temperature) components [35]. The dynamical signal is generally difficult to estimate [36]. We have not determined the cause of the winter circulation trends, which could be tied to internal variability [33], but this observed emerging trend helps constraining the dynamical component in the event attribution process.

Conflicts of Interest

The authors declare that there are no conflicts of interest regarding the publication of this paper.

Authors' Contributions

Pascal Yiou and Robert Vautard designed the analysis on analogue networks. Pascal Yiou produced the figures and drafted

manuscript. All coauthors contributed to the manuscript and figure design.

Acknowledgments

It is a pleasure to thank C. Cassou for discussions at an early stage of this research. This paper was supported by ERC Grant no. 338965-A2C2 and a grant from the French Ministry of Environment (Extremoscope).

References

- [1] J. Cattiaux, R. Vautard, C. Cassou, P. Yiou, V. Masson-Delmotte, and F. Codron, “Winter 2010 in Europe: A cold extreme in a warming climate,” *Geophysical Research Letters*, vol. 37, no. 20, Article ID L20704, 2010.
- [2] J. Cohen, J. Foster, M. Barlow, K. Saito, and J. Jones, “Winter 2009–2010: A case study of an extreme Arctic Oscillation event,” *Geophysical Research Letters*, vol. 37, no. 17, Article ID L17707, 2010.
- [3] J. Cattiaux, R. Vautard, and P. Yiou, “Origins of the extremely warm European fall of 2006,” *Geophysical Research Letters*, vol. 36, no. 6, Article ID L06713, 2009.
- [4] P. Yiou, R. Vautard, P. Naveau, and C. Cassou, “Inconsistency between atmospheric dynamics and temperatures during the exceptional 2006/2007 fall/winter and recent warming in Europe,” *Geophysical Research Letters*, vol. 34, no. 21, Article ID L21808, 2007.
- [5] C. Huntingford, T. Marsh, A. A. Scaife et al., “Potential influences on the United Kingdom’s floods of winter 2013/14,” *Nature Climate Change*, vol. 4, no. 9, pp. 769–777, 2014.
- [6] G. J. Van Oldenborgh, D. B. Stephenson, A. Sterl et al., “Drivers of the 2013/14 winter floods in the UK,” *Nature Climate Change*, vol. 5, no. 6, pp. 490–491, 2015.
- [7] J. A. Francis and S. J. Vavrus, “Evidence linking Arctic amplification to extreme weather in mid-latitudes,” *Geophysical Research Letters*, vol. 39, Article ID L06801, 2012.
- [8] V. Petoukhov, S. Rahmstorf, S. Petri, and H. J. Schellnhuber, “Quasiresonant amplification of planetary waves and recent Northern Hemisphere weather extremes,” *Proceedings of the National Academy of Sciences of the United States of America*, vol. 110, no. 14, pp. 5336–5341, 2013.
- [9] E. A. Barnes, “Revisiting the evidence linking Arctic amplification to extreme weather in midlatitudes,” *Geophysical Research Letters*, vol. 40, no. 17, pp. 4734–4739, 2013.
- [10] J. A. Screen, I. Simmonds, C. Deser, and R. Tomas, “The atmospheric response to three decades of observed arctic sea ice loss,” *Journal of Climate*, vol. 26, no. 4, pp. 1230–1248, 2013.
- [11] J. A. Screen and I. Simmonds, “Caution needed when linking weather extremes to amplified planetary waves,” *Proceedings of the National Academy of Sciences of the United States of America*, vol. 110, no. 26, p. E2327, 2013.
- [12] B. J. Hoskins and I. N. James, *Fluid Dynamics of the Mid-Latitude Atmosphere*, John Wiley and Sons, J, 2014.
- [13] V. Petoukhov, S. Petri, S. Rahmstorf, D. Coumou, K. Kornhuber, and H. J. Schellnhuber, “Role of quasiresonant planetary wave dynamics in recent boreal spring-to-autumn extreme events,” *Proceedings of the National Academy of Sciences of the United States of America*, vol. 113, no. 25, pp. 6862–6867, 2016.

- [14] D. Faranda, G. Masato, N. Moloney et al., “The switching between zonal and blocked mid-latitude atmospheric circulation: a dynamical system perspective,” *Climate Dynamics*, vol. 47, no. 5-6, pp. 1587–1599, 2016.
- [15] D. Faranda, G. Messori, and P. Yiou, “Dynamical proxies of North Atlantic predictability and extremes,” *Scientific Reports*, vol. 7, Article ID 41278, 2017.
- [16] E. N. Lorenz, “Atmospheric predictability as revealed by naturally occurring analogs,” *Journal of the Atmospheric Sciences*, vol. 26, no. 4, pp. 636–646, 1969.
- [17] V. Lucarini, D. Faranda, A. C. G. M. M. de Freitas et al., *Extremes and Recurrence in Dynamical Systems*, John Wiley & Sons, Hoboken, NJ, USA, 2016.
- [18] N. Marwan, M. Carmen Romano, M. Thiel, and J. Kurths, “Recurrence plots for the analysis of complex systems,” *Physics Reports*, vol. 438, no. 5-6, pp. 237–329, 2007.
- [19] J.-P. Eckmann, S. Oliffson Kamphorst, and D. Ruelle, “Recurrence plots of dynamical systems,” *EPL (Europhysics Letters)*, vol. 4, no. 9, pp. 973–977, 1987.
- [20] R. V. Donner, M. Small, J. F. Donges et al., “Recurrence-based time series analysis by means of complex network methods,” *International Journal of Bifurcation and Chaos*, vol. 21, no. 4, pp. 1019–1046, 2011.
- [21] R. Kistler, E. Kalnay, W. Collins et al., “The NCEP-NCAR 50-year reanalysis: monthly means CD-ROM and documentation,” *Bulletin of the American Meteorological Society*, vol. 82, no. 2, pp. 247–267, 2001.
- [22] G. Sturaro, “A closer look at the climatological discontinuities present in the NCEP/NCAR reanalysis temperature due to the introduction of satellite data,” *Climate Dynamics*, vol. 21, no. 3-4, pp. 309–316, 2003.
- [23] W. J. R. M. Priyadarshana and G. Sofronov, “Multiple Break-Points Detection in Array CGH Data via the Cross-Entropy Method,” *IEEE Transactions on Computational Biology and Bioinformatics*, vol. 12, no. 2, pp. 487–498, 2015.
- [24] P. Yiou, T. Salameh, P. Drobinski, L. Menut, R. Vautard, and M. Vrac, “Ensemble reconstruction of the atmospheric column from surface pressure using analogues,” *Climate Dynamics*, vol. 41, no. 5-6, pp. 1333–1344, 2013.
- [25] C. Cassou, L. Terray, and A. S. Phillips, “Tropical Atlantic influence on European heat waves,” *Journal of Climate*, vol. 18, no. 15, pp. 2805–2811, 2005.
- [26] S. Corti, F. Molteni, and T. N. Palmer, “Signature of recent climate change in frequencies of natural atmospheric circulation regimes,” *Letters to Nature*, vol. 398, no. 6730, pp. 799–802, 1999.
- [27] P.-A. Michelangeli, R. Vautard, and B. Legras, “Weather regimes: recurrence and quasi stationarity,” *Journal of the Atmospheric Sciences*, vol. 52, no. 8, pp. 1237–1256, 1995.
- [28] H. von Storch and F. W. Zwiers, *Statistical Analysis in Climate Research*, Cambridge University Press, Cambridge, UK, 1999.
- [29] P. Yiou, K. Goubanova, Z. X. Li, and M. Nogaj, “Weather regime dependence of extreme value statistics for summer temperature and precipitation,” *Nonlinear Processes in Geophysics*, vol. 15, no. 3, pp. 365–378, 2008.
- [30] N. Marwan and J. Kurths, “Line structures in recurrence plots,” *Physics Letters A*, vol. 336, no. 4-5, pp. 349–357, 2005.
- [31] N. Schaller, A. L. Kay, R. Lamb et al., “Human influence on climate in the 2014 southern England winter floods and their impacts,” *Nature Climate Change*, vol. 6, no. 6, pp. 627–634, 2016.
- [32] G. P. Compo, J. S. Whitaker, P. D. Sardeshmukh et al., “The twentieth century reanalysis project,” *Quarterly Journal of the Royal Meteorological Society*, vol. 137, no. 654, pp. 1–28, 2011.
- [33] J. Cattiaux, Y. Peings, D. Saint-Martin, N. Trou-Kechout, and S. J. Vavrus, “Sinuosity of midlatitude atmospheric flow in a warming world,” *Geophysical Research Letters*, vol. 43, no. 15, pp. 8259–8268, 2016.
- [34] G. A. Schmidt, J. D. Annan, P. J. Bartlein et al., “Using palaeoclimate comparisons to constrain future projections in CMIP5,” *Climate of the Past*, vol. 10, no. 1, pp. 221–250, 2014.
- [35] National Academies of Sciences Engineering and Medicine, *Attribution of Extreme Weather Events in the Context of Climate Change*, The National Academies Press, Washington, DC, USA, 2016.
- [36] T. G. Shepherd, “A common framework for approaches to extreme event attribution,” *Current Climate Change Reports*, vol. 2, no. 1, pp. 28–38, 2016.

